

A Multidisciplinary Effort against COVID-19: New Virus, Innovative Solutions

Guilherme C. Tremiliosi¹, Luiz Gustavo P. Simoes¹, Daniel T. Minozzi¹, Renato I. Santos¹, Daiane C. B. Vilela¹, Edison Luiz Durigon², Rafael Rahal Guaragna Machado², Douglas Sales Medina², Lara Kelly Ribeiro³, Ieda Lucia Viana Rosa³, Marcelo Assis³, Juan Andrés⁴, Elson Longo³ and Lucio H. Freitas-Junior²

¹ Nanox Tecnologia S/A, São Carlos, Brazil

² Department of Microbiology, Institute of Biomedical Sciences, ICB, University of São Paulo, Brazil.

³ Center for the Development of Functional Materials, CDMF, Federal University of São Carlos, Brazil

⁴ Laboratory of Theoretical and Computational Chemistry, Department of Analytical and Physical Chemistry, University Jaume I, Spain

As a results of a multidisciplinary R&D&i project carried out in collaboration among the company NANOX TECNOLOGIA, the Institute of Biomedical Sciences, ICB, the Laboratory of Theoretical and Computational Chemistry, QTC, at Universitat Jaume I (Spain), and Center for the Development of Functional Material, CDMF, at São Carlos (Brazil) an innovative material that inactivates COVID-19 by contact has been developed.

NANOX TECNOLOGIA, ICB, QTC, and CDMF have demonstrated a synergistic assembly strategy for the scalable fabrication of antibacterial, fungicide and antiviral materials based on silver nanoparticles (AgNPs). Incorporating AgNPs in a textile fabric is a feasible strategy for promoting antibacterial, fungicide and antiviral activity. With their fast production, ease of activity storing, long-term durability, and high biocidal efficacy, the materials can rapidly and effectively kill bacteria, fungi and viruses. We have also demonstrated that the incorporation of these materials as a biocidal surface protective layer on a textile fabric is capable of achieving robust bioprotection against pathogens.

New Virus

Pathogenic microbes are becoming a potential threat to the health of human beings and environment worldwide. Today, the humanity has experienced epidemic diseases caused by both new and well known viruses, including hepatitis C, HIV/AIDS, SARS-CoV, MERS, Lassa fever, Zika virus, and Ebola virus, as well as Yellow Fever, Influenza, and Measles virus, which are more widespread but can be severe, despite the availability of vaccines.¹ Severe acute respiratory syndrome coronavirus 2 (SARS-CoV-2) is a novel coronavirus that causes the coronavirus disease 2019 (COVID-19). Since its first detection in December 2019,² it has affected millions of people worldwide, carrying a mortality rate much higher than the common flu. These public health outbreaks driven by emerging COVID-19 infectious diseases constitute the forefront of global safety concerns and significant burden on global economies. While there is an urgent need for its effective treatment based on antivirals and vaccines, it is imperative to explore any other effective intervention strategies that may reduce the mortality and morbidity rates of this disease.

In the absence of an effective vaccine, it is expected that not only the current pandemic will continue for several months, but other outbreaks caused by SARS-CoV-2 may take place in the future, in the coming months or years.³ Furthermore, unknown viruses and/or pathogens will likely emerge again, and their pathogenicity, spread,

contagion, and mechanism of action will be inquired. This current global crisis allows us to that we urgently need to prepare ourselves for a new and unpredictable epidemic in the future.

The human body is a diverse ecosystem that harbors hundreds of trillions of microbes (bacteria, fungi and viruses)⁴ that might be or become pathogenic under certain circumstances. The development of innovative materials capable of avoiding the transmission, spread, and entry of these pathogens into the human body is currently in the spotlight. The synthesis of these materials is gaining momentum as methods are providing nontoxic and environmentally acceptable “green chemistry” procedures.

Often, the surface of a material is the medium by which the human body interacts with microbes. Therefore, anti-pathogen strategies based on chemical modification of the material surface have been developed. One procedure is to form a layer on the surface of the material, thereby reducing the chance of contact between the pathogen and the surface of the material. This greatly reduces the number of pathogens adhering to the surface. Another strategy is that killing the adhered pathogen directly by decorating the surface of the material with the biocide agent.

Use of personal protective equipment is considered to be one of the most important strategies for protecting from transmissible pathogens, particularly when aerosol transmission occurs and when no effective treatment or prophylaxis is available for the disease provoked by these pathogens in question. In the case of COVID-19, for instance, the WHO has recently issued recommendation for widespread use of face masks as an important tool in the control of SARS-CoV-2 spread.⁵ Therefore, the current worldwide public health crisis of COVID-19 has highlighted the particularly emergent need for materials that inactivate enveloped viruses on contact for preventing transmission.

New product

Inorganic biocide surfaces and materials have attracted much attention due to their better stability and safety as compared with organic reagents for preventing infections and transmission. Among inorganic agents, silver cation and metal are most widely used. However, Ag cations tend to react with Cl^- , HS^- , and SO_4^{2-} in aqueous solution, forming precipitates, thus losing their biocide activity, which affects the practical application of Ag-loaded biocide agents to a certain extent. Silver and its compounds have been widely used since from ancient time, in 1000 BC, to prevent bacterial growth and wound infections, and make water potable.⁶

Silver metal is a precious metal and is easily discolored under light and heat, but for many years, it was used as medical treatment as a broad-spectrum antibacterial compound before the discovery of antibiotics in the early 20th century.^{7,8} Nanotechnology is capable of modifying silver cation and metal into their nano range, which dramatically changes their chemical and physical properties. Silver nanoparticles (AgNPs) acquire special attention due to its specificity and environment friendly approach with a wide application in industry and medicine due to its antibacterial, antifungal, larvicidal and anti-parasitic characters. The use of AgNPs has been greatly enhanced due to the development of antibiotic resistance against several pathogenic bacteria, and they are employed in biomedical industry as coatings in dressings, in medicinal devices, in the form of nanogels in cosmetics and lotions, etc.^{6,9,10}

According to the literature, there are plenty of protocols focused on the production of hybrid/composite materials based on AgNPs, whose architecture is driven by different synthetic methods and reaction mechanisms.¹¹⁻¹⁷ While the precise reasons for this unique chemistry and physics are unknown, the observed structures, their reproducibility, and synthetic control this reaction offers, there is plenty of room to find innovative possibilities for new technologies.^{18,19}

The silver nanoparticles have been proven to be most useful because they have excellent antimicrobial properties against lethal viruses, microbes/germs, and other microorganisms. These nanoparticles are certainly the most extensively utilized material among all. Thus, it has been used as antimicrobial agent in different textile industries.²⁰ The noble metal nanoparticles are considered as more specific and multipurpose agents with a diversity of biomedical applications considering their use in extremely sensitive investigative assays, radiotherapy enhancement, gene delivery, thermal ablation, and drug delivery. These metallic nanoparticles are also considered to be nontoxic in case of gene and drug delivery applications. Thus, metallic nanoparticles can offer diagnostic and therapeutic possibilities simultaneously.¹⁶

The purpose of this work is to present an innovative material with high bactericide, fungicide and virucide efficiency in their incorporation and application in textile applications such as cotton-based materials that make special biopolymer hosts for composite materials. Finally, it is important to study the reliability of sintered AgNPs, to test and analyze its allergic response, dermatological photoirritant and photosensitive effects, as well as their antimicrobial, fungicide and antiviral activity

EXPERIMENTAL: MATERIALS AND METHODS

Application of chemical finishing onto fabrics

A fine-medium weight 67% polyester /33% cotton woven fabric (plain weave, 120 g/m²; width 1,60m; ends 35/cm; picks 26/cm; yarn Ne 36 67%Polyester / 33% cotton) purchased from local suppliers (São Carlos/SP, Brazil) was used for the application purpose. The antimicrobial products NanoxClean® Ag+Fresh 5K and NanoxClean® Ag+Fresh Hybrid, provided by Nanox Tecnologia S.A. (São Carlos/SP - Brazil), were applied on the polycotton fabric using pad-dry-cure method. The polycotton fabric cut to the size of 30x30 cm was immersed in the solution containing 5% (% weight basis) of Ag+Fresh 5K or Ag+Fresh Hybrid and 6% of Denim 50GL acrylic binder (% weight basis), provided by Star Colours LTDA. (Americana/SP, Brazil), for 5 minutes and passed through a laboratory scale padder, with a 72% wet pick-up maintained for all the treatments. After drying (80°C, 3 min) the fabric was annealed at 170°C for 3 min, then washed with deionized water and then dried at 80°C for 3 min in a ventilated oven. All samples were then conditioned at 25°C and 65% relative humidity for 48h.

Characterization

Micro-Raman spectroscopy was performed using an iHR550 spectrometer (Horiba Jobin-Yvon, Japan) coupled to a charge-coupled device (CCD) detector and an argon-ion laser (Melles Griot, United States) operating at $\lambda = 514.5$ nm and 200 mW. The spectra were carried out in the range of 100-3500 cm⁻¹. Morphologies of the composites were analyzed by Field Emission Scanning Electron Microscopy (FE-SEM) on a FEI instrument (Model Inspect F50) operating at 1 kV. Fourier Transform Infrared Spectroscopy (FTIR) was performed using a Jasco FT/IR-6200 (Japan) spectrophotometer operated in absorbance mode at room temperature. The spectra were carried out in the range of 400-4000 cm⁻¹.

Assessment of Allergic Response

A Human Repeat Insult Patch Test (HRIPT) was performed to determine the absence of the potential for dermal irritability and sensitization of the treated fabrics. The study was carried out in maximized conditions, in which semi-occlusive dressings containing the investigational product and controls were applied to the participants' backs. The application of the study dressings occurred for six weeks, with three weeks

of application alternately, two weeks of rest and a new application of the dressing containing the product in virgin area in the sixth week (challenge). The readings of the application site were performed at each dressing change according to the reading scale recommended by the International Contact Dermatitis Research Group (ICDRG)²¹. Dermatological evaluations were carried out at the beginning and end of the study, and a physician was available for evaluation and assistance to the participants in case of positive or adverse reaction. Participants of both genders, with phototypes III to IV (Fitzpatrick),²² aged between 21 and 70 were selected. The selected participants were distributed as shown in the Table 1.

Table 1. Distribution of selected participants for the HRIPT.

Evaluation Test	Number of Participants	Gender		Age	
		Female	Male	Minimum	Maximum
Primary Dermal Irritability	51	40	11	21	70
Accumulated Dermal Irritability	51	40	11	21	70
Dermal Sensitization	51	40	11	21	70

Assessment of Dermatological Photoirritant and Photosensitive Potential

Since exposure to solar radiation can trigger or aggravate adverse reactions to topical products, knowing the behavior of the product on human skin stimulated with ultraviolet radiation is of fundamental importance for proof of safety. Therefore, a unicentric, blind, comparative clinical study to assess the photoirritating and photosensitizing potential was also conducted, with the aim of proving the absence of the irritating potential of the product applied to the skin when exposed to ultraviolet radiation. The study was carried out with dressings containing the product, applied to the participants' skin and, after removal, controlled irradiation with a spectrum of ultraviolet radiation emission was performed. Readings were performed according to the reading scale recommended by the ICDRG. The study with the participants lasted for five weeks, covering 3 phases: induction, rest and challenge. Dermatological evaluations were performed at the beginning and end of the study, or when there was an indication of positivity or adverse reaction. Participants of both genders, with phototype III (Fitzpatrick), aged between 21 and 62 were selected. The selected participants were distributed as shown in the Table 2.

Table 2. Distribution of selected participants for the photoirritating and photosensitizing clinical study.

Evaluation Test	Number of Participants	Gender		Age	
		Female	Male	Minimum	Maximum
Photosensitization	25	20	05	19	62
Photoirritation	25	20	05	19	62

Assessment of Antimicrobial Activity

The AATCC 147 Parallel Streak Standard Method²³ was used as a qualitative method to evaluate antibacterial activity of the treated fabrics. Sterile plate count agar was dispensed in petri plates. 24 hours broth cultures of the test organisms (*Escherichia Coli* (*E. coli* - ATCC8739) and *Staphylococcus aureus* (*S. aureus* - ATCC6538) were used as inoculums. Using a 10µL inoculation loop, 1 loop full of culture was loaded and

transferred to the surface of the agar plate by making 7.5cm long parallel streaks 1 cm apart in the center of the plate, refilling the loop at every streak. The test specimen was gently pressed transversely, across the five inoculums of streaks to ensure intimate contact with the agar surface. The plates were incubated at 37°C for 18-48 hours. After incubation, a streak of interrupted growth underneath and along the side of the test material indicates antibacterial effectiveness of the fabric.

The quantitative antimicrobial activity assessment of the treated polycotton fabrics was determined according to AATCC Test Method 100²⁴. Fabric specimens (circular swatch 4.8 cm in diameter) were impregnated with 1.0 mL of inoculum in a 250 mL container. The inoculum was a nutrient broth culture containing 2.0~3.0 · 10⁵/mL colony forming units of microorganisms. *E. coli* and *S. aureus* were used as a reference for gram-negative and gram-positive bacteria, respectively, and *C. albicans* (ATCC 10231) as a reference for fungus. The microorganisms counted on the treated polycotton fabric and those on a controlled sample were determined after a 24-hour incubation period at 37°C. The antimicrobial activity was expressed in terms of percentage reduction of the microorganism after contact with the test specimen compared to the number of microbial cells surviving after contact with the control. The results are expressed as percent reduction of microorganisms by Eq. (1).

$$\text{Reduction (\%)} = [(B-A)/B] \times 100 \quad (1)$$

where A and B are the numbers of bacteria or fungus recovered from the antimicrobial-treated and untreated polycotton fabrics in the jar incubated over the desired contact period, respectively.

Assessment of Antiviral Activity

An adaptation of ISO 18184 Determination of antiviral activity of textile products Standard Method²⁵ was used as a reference for a quantitative method to evaluate the treated polycotton's ability to inactivate the SARS-CoV-2 virus particles (SARS-CoV-2/human/BRA/SP02cc/2020 - MT350282), under the tested conditions, at two different time intervals (2 and 5 minutes of contact time). The virus was inoculated into liquid media containing no fabric, treated and non-treated polycotton samples and incubated for 2 different time periods. Then, they were plated onto tissue cultures of Vero CCL-81 cells. After the incubation, the viral genetic material was quantified in each condition using real-time quantitative PCR, and based on the control samples, the ability of each sample to inactivate SARS-CoV-2 was determined.

Briefly, Vero CCL-81 cells were plated onto 24-well plates at 1 × 10⁵ cells per well. The cells were maintained in DMEM high glucose culture medium (Sigma-Aldrich, 51435C) supplemented with 10% fetal bovine serum, 100 U/mL of penicillin, and 100 µg/mL of streptomycin. The plate was incubated at 37 °C, 5% CO₂ atmosphere for 24 h. Following this period, the medium was removed and replaced with 666.7 µL of DMEM High Glucose/well without supplementation.

Three test specimens, non-treated polycotton control and Ag-based antimicrobial treated polycotton samples, measuring 6.25 cm² apiece, were tested. Each test specimen was placed into a different tube and 1.33 mL of DMEM high glucose medium without supplementation was added to each tube. In parallel, 500 µL of culture medium containing SARS-CoV-2 was diluted in 4.5 mL of DMEM medium without supplementation, and then 333.4 µL of this viral suspension was added to each of the tubes containing the pieces of cloth. The mixtures were incubated with the virus for 2 min and the tubes were homogenized every 30 seconds. After this period, 166.7 µL of each sample was transferred to different wells of the plates containing the cells previously seeded. After a total of 5 min of incubation, an additional 166.7 µL-aliquot

was removed from each tube and incubated in other wells on the same plate. As control, the viral suspension was incubated in media without supplementation, with samples collected at 2 and 5 min used to infect Vero cells on the same plate

The plate was incubated for 2 h at 37 °C, 5% CO₂ for viral adsorption, and after this period, 166.6 µL of DMEM High Glucose medium containing 12% fetal bovine serum were added to each well, making to a final volume of 1 mL of medium/well containing 2% serum. Immediately after adding the medium, the plate was further incubated at 37 °C, 5% CO₂. After 48 h, the plate was removed from the incubator and 100 µL of the medium from each well (each well a different condition) was removed and placed in lysis buffer to proceed with the viral RNA extraction. For the extraction, the MagMAX™ CORE Nucleic Acid Purification Kit (Thermo Fisher) was used, following the manufacturer's instructions, on the semi-automated platform MagMAX Express-96 (Applied Biosystems, Weiterstadt, Germany). The detection of viral RNA was carried out using the AgPath-ID One-Step RT-PCR Kit (Applied Biosystems) on an ABI 7500 SDS real-time PCR machine (Applied Biosystems), using a published protocol and sequence of primers and probe for E gene.²⁶ The number of RNA copies/mL was quantified by real-time RT-qPCR using a specific in vitro-transcribed RNA quantification standard, kindly granted by Christian Drosten, Charité - Universitätsmedizin Berlin, Germany, as described previously.²⁷ The viricidal activity, or viral inactivation, was determined as a percentage related to the control (media without fabric specimen).

The experiment was repeated using the same experimental conditions, but with media incubated with two pieces of test specimens (instead of one) per condition.

RESULTS

In order to analyze the local structural order/disorder caused by the addition of Ag-based antimicrobials to polycotton, micro-Raman analyzes were performed. The results are presented in Figure 1. Since the main component of polycotton is cotton (formed by glucose monomers) and polyester (polyethylene terephthalate), the vibrations refer to C, O and H bonds. The cotton Raman spectra of the samples can be divided into four blocks related to the glycosidic ring skeleton, to OH groups, the CH and CH₂ groups and acetylation of cotton. The glycosidic ring presents the fingerprint of the cotton Raman spectra. These modes can be observed at 859, 1104, 1123 and 1183 cm⁻¹ and represent the symmetrical stretching of C-O-C in the plane, asymmetric and symmetrical stretching of C-O-C in the glycosidic link, and asymmetric stretching of C-C ring breathing.²⁸ The presence of OH groups in the samples is observed by the modes located at 287 and 1464 cm⁻¹, related to the twisting and deformation of the C-OH bonds.^{29,30} Four modes related to CH₂ deformations and twisting are observed in 1000, 1291, 1372 and 1418 cm⁻¹. There is still a mode located at 289 cm⁻¹ regarding the twisting of the C-CH bond.³¹ The acetylation of the cotton used is further confirmed by the modes located at 705 and 795 cm⁻¹, referring to deformation O-C=O and the stretching of the H₃C-C bonds.³² Like cotton, polyester has its fingerprint given by the modes referring to its aromatic ring and its esters. It is observed in 1613 cm⁻¹ the mode referring to the stretching of the C¹-C⁴ carbon of the aromatic polyester ring, as well as its CH stretching in 3078 cm⁻¹.^{33,34} It is also possible to observe in 1730 cm⁻¹ the stretching of the C=O bonds of the esters and the stretching of the CH bonds of the methyl groups external to the ring, in 2975 cm⁻¹.³³⁻³⁵ It is observed that the addition of Ag-based antimicrobials do not cause significant changes in the polycotton structure at short-range.

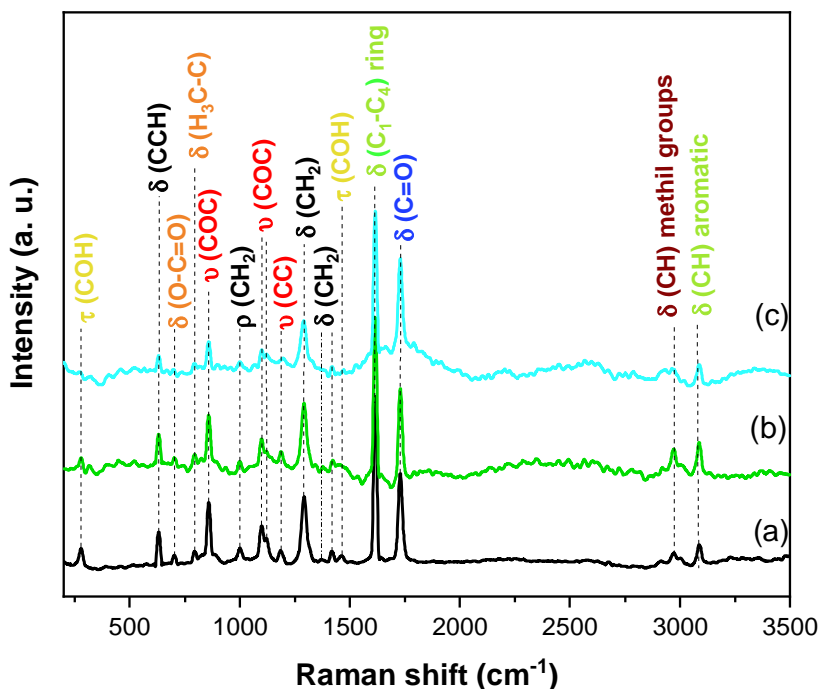


Figure 1. Micro Raman spectra of (a) non-treated polycotton, (b) Ag+Fresh 5k polycotton and (c) Ag+Fresh Hybrid polycotton samples.

As a complementary analysis to micro Raman spectroscopy, FTIR measurements were performed to investigate the functional groups of products after the incorporation of Ag+Fresh 5K and Ag+Fresh Hybrid in the polycotton (Figure 2). It is observed in the samples of pure polycotton and those modified with Ag-based antimicrobials the peaks located at 3540, 2936, 2124, 1947, 1710, 1338, 1147, 832 and 647 cm^{-1} . The peaks located at 3540, 2936 and 2124 cm^{-1} refer to OH stretching and CH deformation respectively, the latter being related to the CH_2 groups of the cellulose structure.^{36,37} The peaks located in 1947, 1710, 1338 and 1147 cm^{-1} correspond respectively to H_2O adsorbed on the polycotton surface, stretching of the CH bond, asymmetric deformation of the C-O-C groups and were attributed to stretching vibrations of intermolecular ester bonding.³⁷⁻³⁹ As in the Raman spectra, the cotton fingerprint can be observed in the FTIR due to the presence of the band located at 832 cm^{-1} , referring to the asymmetric stretching of the glycosidic ring, especially the $\text{C}^1\text{-O-C}^4$ bonds.³⁸ It is observed for the modified polycotton in relation to the non-treated polycotton the displacement of the band located at 1338 cm^{-1} , as well as the decrease of the band located around 647 cm^{-1} , referent to in-plane bending of O-H mode from the glycosidic units and deformation of the OH, respectively.^{40,41} These shifts, as well as the appearance of new bands in the FTIR spectra of the modified polycotton are due to interactions between polycotton and Ag-based antimicrobial additives.⁴²⁻⁴⁴

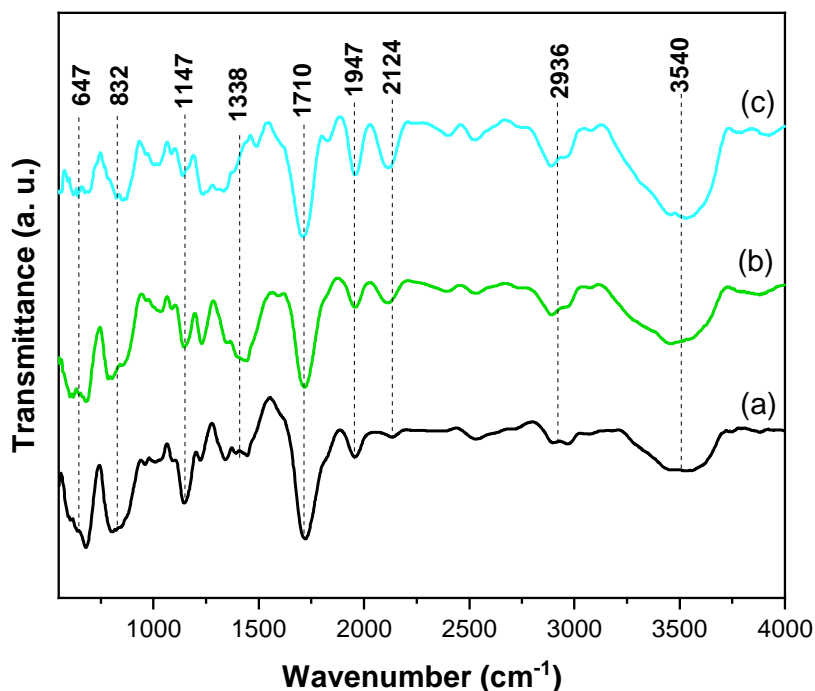


Figure 2. FTIR spectra of (a) non-treated polycotton, (b) Ag+Fresh 5k polycotton and (c) Ag+Fresh Hybrid polycotton samples.

To observe morphological changes in polycotton fibers, FE-SEM measurements were performed (Figure 3). There are no significant differences in the fiber diameters of the samples, being the average diameter values obtained for the non-treated polycotton, Ag+Fresh 5k polycotton and Ag+Fresh Hybrid polycotton samples were 10.62 ± 2.30 , 10.22 ± 2.04 and 10.59 ± 2.50 μm respectively. For Ag+Fresh 5k polycotton (Figures 3d-f), it is possible to observe the formation of small Ag nanoparticles on the polycotton surface, with average size of the 23.51 ± 5.18 nm. Similar behavior was obtained by several other authors in works that incorporated AgNPs into polycotton in different ways.⁴⁵⁻⁵² For the Ag+Fresh Hybrid polycotton sample, the formation of a smaller amount of Ag nanoparticles with average size higher (126.9 ± 19.5 nm) than the than the Ag+Fresh 5K polycotton sample were observed. In addition, there is a homogeneous distribution of micrometric crystals with well-defined morphology over all polycotton surface fibers, with an average size of 1.62 ± 0.44 μm . These differences are due to the different composition of both Ag-based antimicrobials, which result in different surface effects on polycotton surface fibers.

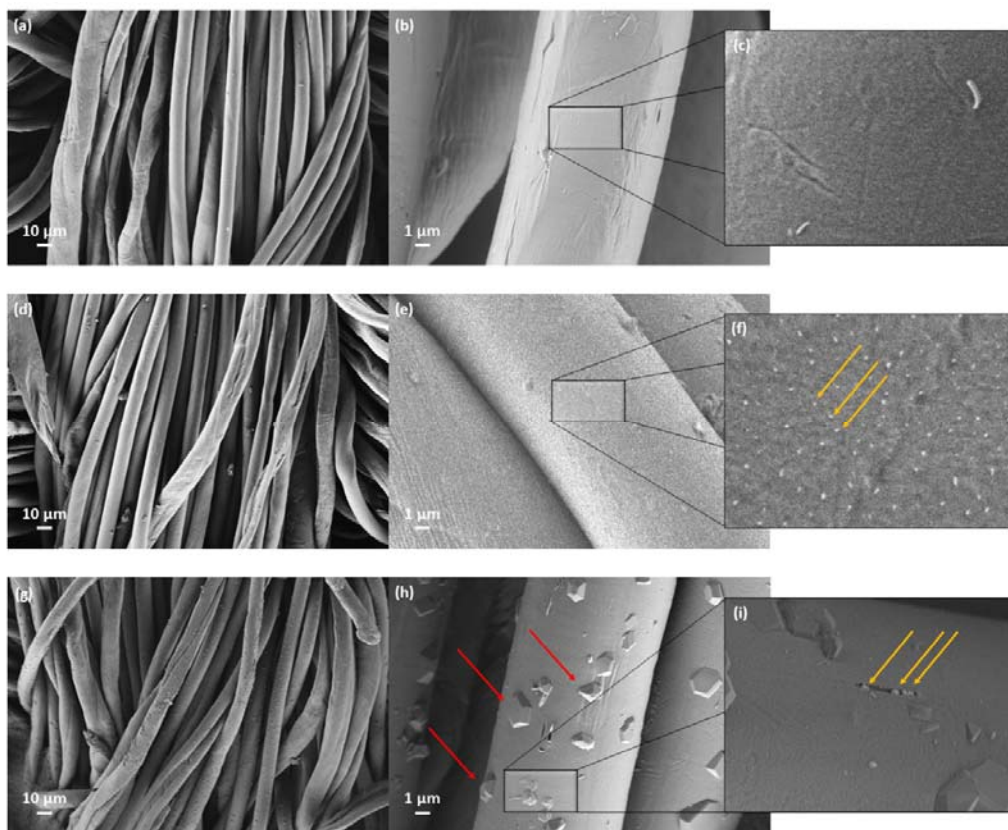


Figure 3. FE-SEM images of (a-c) non-treated polycotton, (d-f) Ag+Fresh 5k polycotton and (g-i) Ag+Fresh Hybrid polycotton samples.

As Ag-based antimicrobial additives caused distinct surface interactions in polycotton fibers, it is expected that this difference will be reflected in their physical, chemical and biological properties. In this sense, experiments were carried out to evaluate the biological properties of composites obtained through the allergenic response to humans and microbicidal activity against *E. coli*, *S. aureus*, *C. albicans* and SARS-CoV-2.

Both the Human Repeat Insult Patch Test and the clinical study to assess the photoirritating and photosensitizing potential were conducted according to the Cosmetic Product Safety Assessment Guide, published by the Brazilian regulatory agency ANVISA⁵³, by the ECOLYZER Group (São Paulo/SP, Brazil), an independent and ISO certified laboratory. For the HRIPT, Primary Dermal Irritability, Accumulated Dermal Irritability and Dermal Sensitization potential were determined. The clinical evaluation criterion was the observation of clinical signs or symptoms such as swelling (edema), redness (erythema), papules and vesicles according to the reading scale recommended by the ICDRG. No adverse reactions (erythema, edema, papules or vesicles) were detected in the product's application areas, in the analysis of primary and accumulated irritability, sensitization, during the study period. The same clinical evaluation criterion was used to determine the Dermal Photoirritation and Dermal Photosensitization in the clinical study. As in the HRIPT, on this study no adverse reactions (erythema, edema, papules or vesicles) were detected in the product's application areas during the study period. According to the results obtained from the sample of participants studied, we can conclude that the treated fabrics did not induce a photoirritating, photosensitizing, irritation nor sensitization process and, therefore, can be considered hypoallergenic and dermatologically tested and approved, being considered safe, according to ANVISA's

The AATCC 147 test results against *S. aureus* (gram positive) and *E. coli* (gram negative) bacteria for the non-treated and the Ag-based antimicrobial treated polycotton samples are shown in Figure 4 and Table 3. For the control polycotton, growth of *E. coli* and *S. aureus* was observed under the specimen while no growth appeared for the treated fabric. The zone of inhibition for the control sample was 0 mm, in comparison to 2-3 mm for the treated fabric. It can be seen from these results that the Ag-based antimicrobials treated fabrics displayed a high level of antibacterial performance.

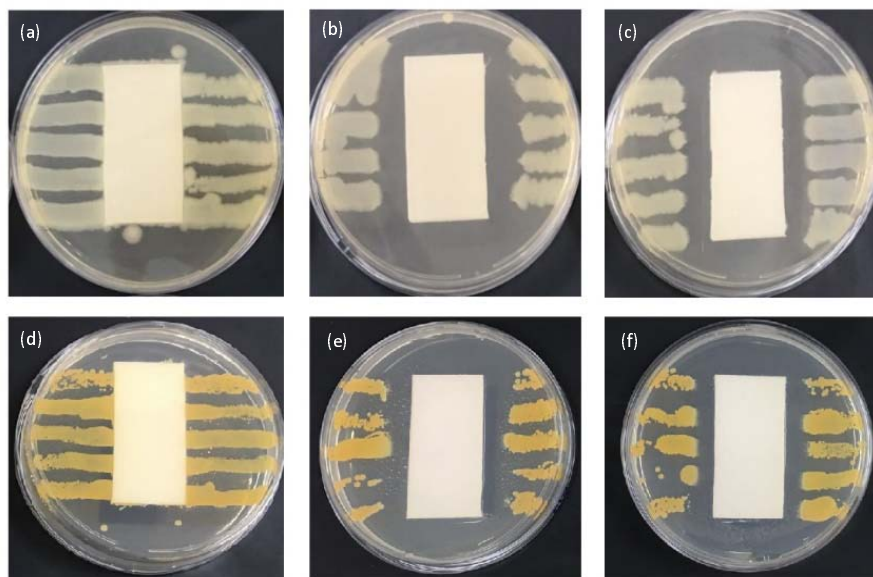


Figure 4. AATCC 147 test result against *E. coli* for a non-treated polycotton sample as a reference (a) and for the Ag-based antimicrobial treated polycotton (b – Ag+Fresh 5k and c – Ag+Fresh Hybrid) and AATCC 147 test result against *S. aureus* for a non-treated polycotton sample as a reference (d) and for the Ag-based antimicrobial treated fabric (e – Ag+Fresh 5k and f – Ag+Fresh Hybrid) exhibiting, respectively, no peripheral inhibition and a measurable zone of inhibition.

Table 3. AATCC 147 tests results against *S. aureus* and *E. coli* for non-treated (control) and Ag-based antimicrobials treated fabric samples.

	<i>E. coli</i>	<i>S. aureus</i>
Antimicrobial Product / Concentration of Antimicrobial in impregnation bath ^a (% weight)	Growth under the specimen	
Non-treated control polycotton / 0	Yes	Yes
Ag+Fresh 5K treated polycotton / 5%	No	No
Ag+Fresh Hybrid treated polycotton / 5%	No	No
	Zone of inhibition (mm)	
Non-treated control polycotton / 0	0	0
Ag+Fresh 5K treated polycotton / 5%	3	2.5
Ag+Fresh Hybrid treated polycotton / 5%	2	2

^a Treatment condition: 5 min soaking time in 5% solution; 72% wet pick-up (padder); 80°C, 3 min drying; annealing at 170°C / 3 min

The quantitative antimicrobial activities of finished textiles treated with the two different Ag-based antimicrobials according to the AATCC 100 standard are shown in

Table 4. All the Ag-based treated polycotton samples had efficient antimicrobial activities, displaying a 99.99% reduction in all tested samples.

Table 4. Quantitative antibacterial results according to the AATCC 100 standard.

Antimicrobial Product / Concentration of Antimicrobial in impregnation bath ^a (% weight)	Microbial Reduction ^b (%)								
	<i>S. aureus</i> ATCC 6538			<i>E. coli</i> ATCC 8739			<i>C. albicans</i> ATCC 10231		
	Zero-time bacteria count	Bacteria count after 24 hours	% Reduction	Zero-time bacteria count	Bacteria count after 24 hours	% Reduction	Zero-time Fungi count	Fungi count after 24 hours	% Reduction
Non-treated Control	2.1 x 10 ⁵	2.2 x 10 ⁵	-	2.3 x 10 ⁵	2.2 x 10 ⁵	-	2.0 x 10 ⁵	2.2 x 10 ⁵	-
Ag+Fresh 5K / 5%	2.1 x 10 ⁵	1.6 x 10	99.99%	2.3 x 10 ⁵	1.3 x 10	99.99%	2.0 x 10 ⁵	1.3 x 10	99.99%
Ag+Fresh Hybrid / 5%	2.1 x 10 ⁵	1.1 x 10	99.99%	2.3 x 10 ⁵	1.1 x 10	99.99%	2.0 x 10 ⁵	1.4 x 10	99.99%

^a Treatment condition: 5 min soaking time in 5% solution; 72% wet pick-up (padder); 80°C, 3 min drying; annealing at 170°C / 3 min;

^b Percent bacterial reduction as measured against a non-treated control.

The antiviral activity test was designed to determine the inactivation of viral particles upon short exposure to the products, which in this case were the Ag-based treated polycotton samples incubated in liquid media. After a short period of incubation, the media were transferred to a cell culture, where viable virions would be able to enter cells and replicate within. The supernatant of cell cultures was recovered after 48 h and the viral load was determined by RT-qPCR, resulting in the determination of number of viral RNA copies per mL.

Table 5 shows the number of copies of the control media without any fabric sample, non-treated polycotton, and the two Ag-based treated polycotton samples at the two different tested time periods. With the result of the number of copies of each sample, the viral inactivation effect of each cloth was calculated, using the media without any fabric sample as control.

Table 5. Copies per mL of SARS-CoV-2 at different times in the first experiment.

Antimicrobial Product / Concentration of Antimicrobial in impregnation bath ^a (% weight)	Copies/mL (SARS-CoV-2)	Viral Inactivation (%)	Incubation
Media without any fabric sample	1.85 × 10 ⁹	-	2 min
Non-treated Control	1.55 × 10 ⁹	16.57%	
Ag+Fresh 5K / 5%	2.48 × 10 ⁸	86.65%	
Ag+Fresh Hybrid / 5%	7.39 × 10 ⁶	99.60%	
Media without any fabric sample	1.26 × 10 ⁹	-	5 min
Non-treated Control	9.87 × 10 ⁸	21.67%	
Ag+Fresh 5K / 5%	2.14 × 10 ⁸	83.12%	
Ag+Fresh Hybrid / 5%	5.50 × 10 ⁷	95.65%	

^a Treatment condition: 5 min soaking time in 5% solution; 72% wet pick-up (padder); 80°C, 3 min drying; annealing at 170°C / 3 min;

Regarding the second experiment, the number of copies per milliliter in each sample was also obtained and the percentage of inhibition of the products was calculated from the control media without any fabric sample. The obtained results were summarized in Table 6.

Table 6. Copies per mL of SARS-CoV-2 at different times in the second experiment.

Antimicrobial Product / Concentration of Antimicrobial in impregnation bath ^a (% weight)	Copies/mL (SARS-CoV-2)	Viral Inactivation (%)	Incubation
Media without any fabric sample	4.15×10^9	-	2 min
Non-treated Control	3.27×10^9	21.28%	
Ag+Fresh 5K / 5%	6.82×10^8	83.57%	
Ag+Fresh Hybrid / 5%	2.72×10^5	99.99%	
Media without any fabric sample	3.03×10^9	-	5 min
Non-treated Control	2.34×10^9	22.77%	
Ag+Fresh 5K / 5%	3.60×10^8	88.12%	
Ag+Fresh Hybrid / 5%	1.04×10^5	99.99%	

^a Treatment condition: 5 min soaking time in 5% solution; 72% wet pick-up (padder); 80°C, 3 min drying; annealing at 170°C / 3 min;

The following graphs represent the data described in Tables 5 and 6, of the control media without any fabric sample, non-treated polycotton, and the two Ag-based treated polycotton samples.

Figures 5 and 6 show the results of the first and second experiments, respectively, indicating the number of viral copies per mL and the percentage of inhibition of each compound above the bar referring to it. Inhibition was calculated for each treatment using its respective control.

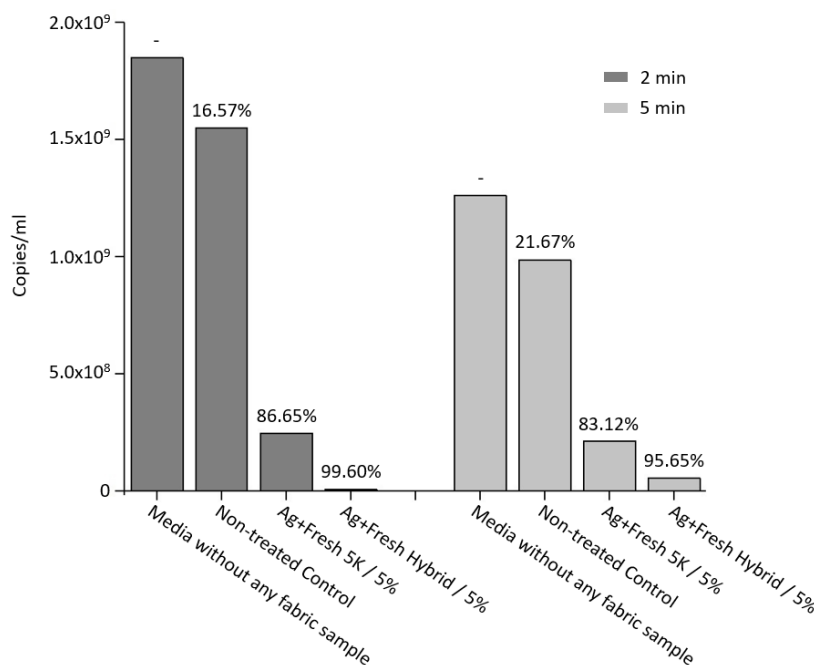


Figure 5. Representative graph of the data obtained in the first experiment, relating the tested products to the viral load found and the percentage of inhibition.

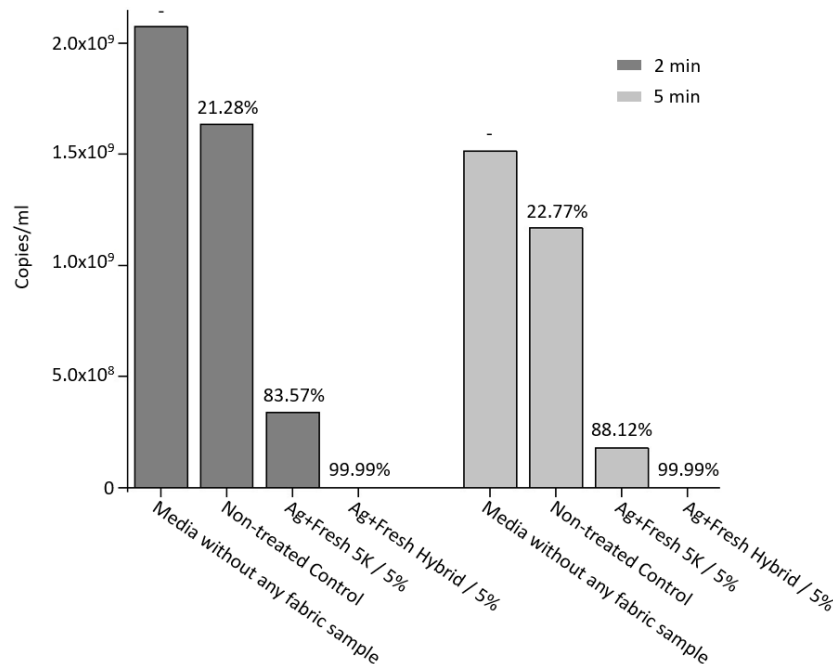


Figure 6. Representative graph of the data obtained in the second experiment, relating the tested products to the viral load found and the percentage of inhibition.

In both experiments, in the two time periods tested, the untreated polycotton showed a subtle activity, which was already expected by data already published by Chin and colleagues.⁵⁴ The Ag+Fresh 5K treated polycotton showed a high viricidal activity when incubated with the virus. At both time periods in both experiments, the Ag+Fresh Hybrid treated polycotton obtained a higher rate of viral inactivation compared to Ag+Fresh 5K.

In short, both treated polycotton samples were effective in viral inhibition in 2 and 5 minutes in two different experiments, where there was variation in the amount of virus per cm² of fabric (4x less virus/cm² in the second experiment). The Ag+Fresh Hybrid treated polycotton showed the best activity, reaching 99.99% within two minutes of incubation with the virus in the second experiment. The Ag+Fresh 5K treated polycotton, despite being less effective than the Ag+Fresh Hybrid treated polycotton, showed high anti-SARS-CoV-2 activity, with more than 80% inhibition rate in all tests performed.

The differential capabilities of this product are the prevention of cross infection caused by pathogens, such as opportunistic bacteria and fungi, responsible for the worsening of COVID-19 and other types of viruses. The fabrication of these devices composed of these fascinating materials may provide new insights into the development of protection materials in a sustainable, self-recharging, and structurally adaptive form. Based on the significant ongoing research and applications, it is expected that these new materials play an outstanding role not only in this type of devices but also in other important areas of applications in the fields of health, energy, water, and environment. Therefore, this product had excellent universality in the preparation of antibacterial, fungicide and antiviral surface on different materials. And their cytocompatibility will open up its avenue to other applications.

The Key: Multidisciplinary Knowledge and Technological Transfer

Deep research and useful technological transfer require not only knowledge but also experience, which can only be obtained with time and practice: they are the qualities necessary to carry out a task with tremendous socioeconomic impact

worldwide. The combined ICB's, QTC's and CDMF's original approach is based on linking theory and simulation to experimentation. This work strategy has allowed to find and design structure–activity relationships and to obtain new physical and chemical properties of materials for specific technological applications. We thus employ quantum mechanics theory, simulations and computational modeling, based on the methods and techniques of theoretical and computational chemistry, to discover even more efficient materials and to design novel and green routes based on our proposed rules. All scientific and technological knowledge, acquired from more than 30 years of collaboration, render as a result the discovery and synthesis of innovative and new multifunctional, nano-, micro- materials with tailored properties, which are employed to solve problems related to renewable energy, health, and the environmental sustainability. In this case the fourth partner is NANOX TECNOLOGIA company.

The discovery of the new materials has enabled to carry out innovation and technology transfer projects with various companies in the province's ceramic, textile and plastic sectors in Castellón (Spain) and São Carlos (Brazil) and with other Spanish, Brazilian, European, North and South American companies. The quality and originality of the results and contributions obtained have caused a paradigm shift both in the terms and in the way that new advanced materials are studied, researched, discovered, synthesized, and applied. With all this, they have managed to achieve an innovative know-how in the development of new technologies. Furthermore, by future combining biocompatible nanofiber matrix and biocides, these materials would open broad technological implications for tissue engineering, photodynamic therapy, catalytic processes, biosensors, bioactuators, medical therapy equipment, and smart wearable devices.

Research on this multidisciplinary field, like any other research, is most effective if it is adequately funded and researchers have the necessary skill sets for gaining deep understanding from every conceivable perspective. This COVID-19 pandemic has become the center of attention for obvious reasons, but this should not detract from attention on other pathogens that will surely arrive. We need research expertise in both basic and applied sciences, including not only health sciences but also technological sciences, social sciences, biology, chemistry, physics, quantum mechanics, materials science, medicine, nanotechnology, engineering, and epidemiology, to maximize the impact and benefit of this targeted research to the community. The multidisciplinary scientific and technological research and development work carried out in the Laboratories of NANOX TECNOLOGIA, ICB, QTC, and CDMF is a clear cut example of how from basic, fundamental and oriented research it is possible to achieve a high scientific, technological, and socioeconomic impact that can, in this case, contribute to synthesizing and applying materials for the design and development of new technologies that minimize the impact of the global epidemic of disease (COVID-19) caused by a novel coronavirus (SARS-CoV-2).

Finally, it is important to remark that the close interplay among theory, simulations and experiment has been critical in developing this innovative material. The prospect of improving our fundamental understanding of the activity mechanisms is becoming a reality. New chemistry and physics and unexpected behavior is now discovered rationalized and applied to solve problems with high socioeconomic impact. As experimental and theoretical techniques are combined in new and exciting ways, and the state-of-the-art advances, it will be possible to examine increasingly complex and interesting systems under different conditions and highlight the prospects for the field.

Despite this impressive progress, it should be noted that this product has only been applied to a very small subset of surfaces (with particularly attractive properties). While applying these products to other surfaces remains an ongoing challenge, progress is already underway. Future studies should be done to evaluate the safety and efficacy

of the prepared products. Since, these technologies have greater scale up capabilities compared to other delivery systems, feasibility of product transfer from research and development to large scale must be determined with the help of technology transfer. All of these reveal significant potential to yield innovative insights for the design of active materials and interfaces.

Acknowledgements

The authors acknowledge the financial support of the Brazilian research financing institutions: Fundação de Amparo à Pesquisa do Estado de São Paulo (FAPESP CEPID-finance code 2013/07296□2, Process 2017/24769-2, Process 2016/20045-7 and PIPE-finance codes 2004/08778-1 and 2017/15924-4), Coordenação de Aperfeiçoamento de Pessoal de Nível Superior - Brasil (CAPES) - Finance Code 001, Conselho Nacional de Desenvolvimento Científico e Tecnológico (CNPq) and Financiadora de Estudos e Projetos (FINEP). J. A. acknowledge Universitat Jaume I for projects UJI-B2016-25 and UJI-B2019-30, and Ministerio de Ciencia, Innovación y Universidades (Spain) project PGC2018-094417-B-I00 for supporting this research financially. We also acknowledge the Servei Informàtica, Universitat Jaume I for a generous allotment of computer time.

References

1. Carrasco-Hernandez, R., Jácome, R., López Vidal, Y. & Ponce de León, S. Are RNA Viruses Candidate Agents for the Next Global Pandemic? A Review. *ILAR J.* **58**, 343–358 (2017).
2. Zhu, N. *et al.* A Novel Coronavirus from Patients with Pneumonia in China, 2019. *N. Engl. J. Med.* **382**, 727–733 (2020).
3. de Wit, E., van Doremalen, N., Falzarano, D. & Munster, V. J. SARS and MERS: recent insights into emerging coronaviruses. *Nat. Rev. Microbiol.* **14**, 523–534 (2016).
4. Sender, R., Fuchs, S. & Milo, R. Revised Estimates for the Number of Human and Bacteria Cells in the Body. *PLOS Biol.* **14**, e1002533 (2016).
5. Organización Mundial de la Salud. Advice on the use of masks in the context of COVID-19: interim guidance-2. *Guía Interna la OMS* 1–5 (2020).
6. Rai, M., Yadav, A. & Gade, A. Silver nanoparticles as a new generation of antimicrobials. *Biotechnol. Adv.* **27**, 76–83 (2009).
7. Barillo, D. J. & Marx, D. E. Silver in medicine: A brief history BC 335 to present. *Burns* **40**, S3–S8 (2014).
8. Alexander, Wesley, J. History of the medical use of silver. *Surg. Infect. (Larchmt)*. **10**, 289–294 (2009).
9. Vardanyan, Z., Gevorkyan, V., Ananyan, M., Vardapetyan, H. & Trchounian, A. Effects of various heavy metal nanoparticles on *Enterococcus hirae* and *Escherichia coli* growth and proton-coupled membrane transport. *J. Nanobiotechnology* **13**, 69 (2015).
10. Rudramurthy, G. R., Swamy, M. K., Sinniah, U. R. & Ghasemzadeh, A. Nanoparticles: Alternatives Against Drug-Resistant Pathogenic Microbes. *Molecules* **21**, (2016).
11. Zhang, P., Jiang, X., Yuan, P., Yan, H. & Yang, D. Silver nanopaste: Synthesis, reinforcements and application. *Int. J. Heat Mass Transf.* **127**, 1048–1069 (2018).
12. Khatoon, N., Mazumder, J. A. & Sardar, M. Biotechnological Applications of Green Synthesized Silver Nanoparticles. *J. Nanosci. Curr. Res.* **02**, (2017).
13. Iravani, S., Korbekandi, H., Mirmohammadi, S. V & Zolfaghari, B. Synthesis of silver nanoparticles: chemical, physical and biological methods. *Res. Pharm. Sci.*

- 9, 385–406 (2014).
14. Abbasi, E. *et al.* Silver nanoparticles: Synthesis methods, bio-applications and properties. *Crit. Rev. Microbiol.* **42**, 173–180 (2016).
 15. Fahmy, H. M. *et al.* Advances in nanotechnology and antibacterial properties of biodegradable food packaging materials. *RSC Adv.* **10**, 20467–20484 (2020).
 16. Yamada, M., Foote, M. & Prow, T. W. Therapeutic gold, silver, and platinum nanoparticles. *WIREs Nanomedicine and Nanobiotechnology* **7**, 428–445 (2015).
 17. Yaqoob, A. A., Umar, K. & Ibrahim, M. N. M. Silver nanoparticles: various methods of synthesis, size affecting factors and their potential applications—a review. *Appl. Nanosci.* **10**, 1369–1378 (2020).
 18. Lara, H. H., Ixtapan-Turrent, L., Jose Yacaman, M. & Lopez-Ribot, J. Inhibition of *Candida auris* Biofilm Formation on Medical and Environmental Surfaces by Silver Nanoparticles. *ACS Appl. Mater. Interfaces* **12**, 21183–21191 (2020).
 19. Gunell, M. *et al.* Antimicrobial characterization of silver nanoparticle-coated surfaces by “touch test” method. *Nanotechnol. Sci. Appl.* **10**, 137–145 (2017).
 20. Hasan, S. A Review on Nanoparticles □: Their Synthesis and Types. *Res. J. Recent Sci. Res. J. Recent. Sci. Uttar Pradesh (Lucknow Campus)* **4**, 1–3 (2014).
 21. Wilkinson, D. S. *et al.* Terminology of contact dermatitis. *Acta Derm. Venereol.* **50**, 287–292 (1970).
 22. Fitzpatrick, T. B. The Validity and Practicality of Sun-Reactive Skin Types I Through VI. *Arch. Dermatol.* **124**, 869–871 (1988).
 23. AATCC 147-2004: Antimicrobial Activity Assessment of Textile Materials: Parallel Streak Method from American Association of Textile Chemists and Colorists. (2006).
 24. AATCC 100-2004: Antibacterial Finishes on Textile Materials: Assessment of Developed from American Association of Textile Chemists and Colorists. (2006).
 25. ISO 18184:2019: Textiles — Determination of antiviral activity of textile products. (2019).
 26. Corman, V. M. *et al.* Detection of 2019 novel coronavirus (2019-nCoV) by real-time RT-PCR. *Euro Surveill. Bull. Eur. sur les Mal. Transm. Eur. Commun. Dis. Bull.* **25**, (2020).
 27. Drosten, C. *et al.* Identification of a novel coronavirus in patients with severe acute respiratory syndrome. *N. Engl. J. Med.* **348**, 1967–1976 (2003).
 28. Rygula, A., Jekiel, K., Szostak-Kot, J., Wrobel, T. P. & Baranska, M. Application of FT-Raman spectroscopy for in situ detection of microorganisms on the surface of textiles. *J. Environ. Monit.* **13**, 2983–2987 (2011).
 29. Cabrales, L., Abidi, N. & Manciu, F. Characterization of developing cotton fibers by confocal Raman microscopy. *Fibers* **2**, 285–294 (2014).
 30. Liu, Y. Vibrational spectroscopic investigation of Australian cotton cellulose fibres Part 1. A Fourier transform Raman study†. *Analyst* **123**, 633–636 (1998).
 31. Was-Gubala, J. & Machnowski, W. Application of Raman Spectroscopy for Differentiation Among Cotton and Viscose Fibers Dyed with Several Dye Classes. *Spectrosc. Lett.* **47**, 527–535 (2014).
 32. Adebajo, M. O., Frost, R. L., Kloprogge, J. T. & Kokot, S. Raman spectroscopic investigation of acetylation of raw cotton. *Spectrochim. Acta Part A Mol. Biomol. Spectrosc.* **64**, 448–453 (2006).
 33. Rebollar, E. *et al.* Physicochemical modifications accompanying UV laser induced surface structures on poly(ethylene terephthalate) and their effect on adhesion of mesenchymal cells. *Phys. Chem. Chem. Phys.* **16**, 17551–17559 (2014).

34. Bauer, A. J. R. Raman Spectroscopy for Fiber Analysis. *Appl. Note Raman* **023**, 3–6 (2018).
35. Lin, C.-C., Krommenhoek, P. J., Watson, S. S. & Gu, X. Chemical depth profiling of photovoltaic backsheets after accelerated laboratory weathering. *Reliab. Photovolt. Cells, Modul. Components, Syst. VII* **9179**, 91790R (2014).
36. Xu, L.-L., Guo, M.-X., Liu, S. & Bian, S.-W. Graphene/cotton composite fabrics as flexible electrode materials for electrochemical capacitors. *RSC Adv.* **5**, 25244–25249 (2015).
37. Fang, L. *et al.* Eco-friendly cationic modification of cotton fabrics for improving utilization of reactive dyes. *RSC Adv.* **5**, 45654–45661 (2015).
38. Chung, C., Lee, M. & Choe, E. K. Characterization of cotton fabric scouring by FT-IR ATR spectroscopy. *Carbohydr. Polym.* **58**, 417–420 (2004).
39. Borazan, A. A. & Gokdai, D. Pine Cone and Boron Compounds Effect as Reinforcement on Mechanical and Flammability Properties of Polyester Composites. *Open Chem.* **16**, 427–436 (2018).
40. Portella, E. H., Romanzini, D., Angrizani, C. C., Amico, S. C. & Zattera, A. J. Influence of Stacking Sequence on the Mechanical and Dynamic Mechanical Properties of Cotton/Glass Fiber Reinforced Polyester Composites. *Mater. Res.* **19**, 542–547 (2016).
41. Al-Balakocy, N., El-Badry, K. & Hassan, T. Multi-Finishing of Polyester and Polyester Cotton Blend Fabrics Activated by Enzymatic Treatment and Loaded with Zinc Oxide Nanoparticles. in (2019). doi:10.5772/intechopen.89750.
42. Xu, Q. *et al.* Antibacterial cotton fabric with enhanced durability prepared using silver nanoparticles and carboxymethyl chitosan. *Carbohydr. Polym.* **177**, 187–193 (2017).
43. Yan, L. *et al.* Synthesis and optical properties of composite films from P3HT and sandwich-like Ag–C–Ag nanoparticles. *RSC Adv.* **5**, 79860–79867 (2015).
44. Liu, H. *et al.* Laundering durable antibacterial cotton fabrics grafted with pomegranate-shaped polymer wrapped in silver nanoparticle aggregations. *Sci. Rep.* **4**, 5920 (2014).
45. Nam, S., Condon, B. D., Delhom, C. D. & Fontenot, K. R. Silver-cotton nanocomposites: Nano-design of microfibrillar structure causes morphological changes and increased tenacity. *Sci. Rep.* **6**, 37320 (2016).
46. Xu, Q. *et al.* Enhancing the surface affinity with silver nano-particles for antibacterial cotton fabric by coating carboxymethyl chitosan and l-cysteine. *Appl. Surf. Sci.* **497**, 143673 (2019).
47. Zhang, F., Wu, X., Chen, Y. & Lin, H. Application of silver nanoparticles to cotton fabric as an antibacterial textile finish. *Fibers Polym.* **10**, 496–501 (2009).
48. Chen, C.-Y. & Chiang, C.-L. Preparation of cotton fibers with antibacterial silver nanoparticles. *Mater. Lett.* **62**, 3607–3609 (2008).
49. Maráková, N. *et al.* Antimicrobial activity and cytotoxicity of cotton fabric coated with conducting polymers, polyaniline or polypyrrole, and with deposited silver nanoparticles. *Appl. Surf. Sci.* **396**, 169–176 (2017).
50. Ghosh, S., Yadav, S. & Reynolds, N. Antibacterial properties of cotton fabric treated with silver nanoparticles. *J. Text. Inst.* **101**, 917–924 (2010).
51. Montazer, M., Alimohammadi, F., Shamei, A. & Rahimi, M. K. Durable antibacterial and cross-linking cotton with colloidal silver nanoparticles and butane tetracarboxylic acid without yellowing. *Colloids Surfaces B Biointerfaces* **89**, 196–202 (2012).
52. Bacciarelli-Ulacha, A., Rybicki, E., Matyjas-Zgondek, E., Pawlaczyk, A. & Szykowska, M. I. A New Method of Finishing of Cotton Fabric by in Situ Synthesis of Silver Nanoparticles. *Ind. Eng. Chem. Res.* **53**, 4147–4155 (2014).

53. Agência Nacional de Vigilância Sanitária. Guia para Avaliação de Segurança de Produtos Cosméticos Guia para Avaliação de Segurança de Produtos Cosméticos. *Anvisa* **2**, 1–74 (2012).
54. Chin, A. W. H. *et al.* Stability of SARS-CoV-2 in different environmental conditions. *The Lancet Microbe* **5247**, 2004973 (2020).